AMERICAN SOCIETY FOR MICROBIOLOGY | Journal of Virology

Genome-Wide Gene Expression Analysis Identifies the Proto-oncogene Tyrosine-Protein Kinase Src as a Crucial Virulence Determinant of Infectious Laryngotracheitis Virus in Chicken Cells

Hai Li, Fengjie Wang, Zongxi Han, Qi Gao, Huixin Li, Yuhao Shao, Nana Sun, Shengwang Liu

Division of Avian Infectious Diseases, State Key Laboratory of Veterinary Biotechnology, Harbin Veterinary Research Institute, the Chinese Academy of Agricultural Sciences, Harbin, People's Republic of China

ABSTRACT

Given the side effects of vaccination against infectious laryngotracheitis (ILT), novel strategies for ILT control and therapy are urgently needed. The modulation of host-virus interactions is a promising strategy to combat the virus; however, the interactions between the host and avian ILT herpesvirus (ILTV) are unclear. Using genome-wide transcriptome studies in combination with a bioinformatic analysis, we identified proto-oncogene tyrosine-protein kinase Src (Src) to be an important modulator of ILTV infection. Src controls the virulence of ILTV and is phosphorylated upon ILTV infection. Functional studies revealed that Src prolongs the survival of host cells by increasing the threshold of virus-induced cell death. Therefore, Src is essential for viral replication *in vitro* and *in ovo* but is not required for ILTV-induced cell death. Furthermore, our results identify a positive-feedback loop between Src and the tyrosine kinase focal adhesion kinase (FAK), which is necessary for the phosphorylation of either Src or FAK and is required for Src to modulate ILTV infection. To the best of our knowledge, we are the first to identify a key host regulator controlling host-ILTV interactions. We believe that our findings have revealed a new potential therapeutic target for ILT control and therapy.

IMPORTANCE

Despite the extensive administration of live attenuated vaccines starting from the mid-20th century and the administration of recombinant vaccines in recent years, infectious laryngotracheitis (ILT) outbreaks due to avian ILT herpesvirus (ILTV) occur worldwide annually. Presently, there are no drugs or control strategies that effectively treat ILT. Targeting of host-virus interactions is considered to be a promising strategy for controlling ILTV infections. However, little is known about the mechanisms governing host-ILTV interactions. The results from our study advance our understanding of host-ILTV interactions on a molecular level and provide experimental evidence that it is possible to control ILT via the manipulation of host-virus interactions.

Infectious laryngotracheitis (ILT) is a major respiratory disease of chickens that is induced by avian ILT herpesvirus (ILTV; also known as gallid herpesvirus 1). ILTV belongs to the *Iltovirus* genus within the *Herpesviridae* family. Infection with ILTV can induce a mild to severe upper respiratory tract disease in chickens, depending on the virulence of the virus, and it causes large economic losses to the poultry industry worldwide annually. Vaccination using live attenuated virus has been the most commonly used method to control ILT outbreaks since the mid-20th century. Vaccination infects naive chickens with live attenuated virus, thereby establishing latent viral carriers; however, it is not recommended that this vaccine be used in regions where ILT outbreaks are absent (1–4). The majority of currently used live attenuated virus vaccines can induce successful protection in chickens (5). New outbreaks of ILT are continually being identified in many countries, especially in regions where live attenuated vaccines have been extensively administered (6). A growing body of evidence from molecular typing data collected worldwide has revealed that the currently used live attenuated vaccine strains could generate, via recombination, a virulent virus that could be the cause of current outbreaks (7–12). Increasing concerns regarding the biosafety of live attenuated ILTV vaccines have triggered the development of recombinant vaccines using viral vectors, and these have been released in some countries (6). However, none of the currently available recombinant vaccines are able to clear latent virus from an infected host. As a consequence, a residual latent infection can induce new outbreaks under certain conditions when host immunity is compromised, such as under stress and at the onset of egg laying (13, 14). Therefore, novel strategies that are independent of the host immune system, such as tighter farm biosecurity and anti-ILTV breeding, are required to control ILT outbreaks. It is hoped that these new strategies that are being developed will improve the control of ILT and reduce the extensive use of live attenuated virus as vaccines.

Received 21 July 2015 **Accepted** 28 September 2015

Accepted manuscript posted online 7 October 2015

Citation Li H, Wang F, Han Z, Gao Q, Li H, Shao Y, Sun N, Liu S. 2016. Genome-wide gene expression analysis identifies the proto-oncogene tyrosine-protein kinase Src as a crucial virulence determinant of infectious laryngotracheitis virus in chicken cells. J Virol 90:9–21. doi:10.1128/JVI.01817-15.

Editor: R. M. Longnecker

Address correspondence to Shengwang Liu, swliu@hvri.ac.cn.

H.L. and F.W. contributed equally to this article.

Supplemental material for this article may be found at http://dx.doi.org/10.1128/JVI.01817-15.

In addition to controlling ILTV infections by establishing cell-extrinsic barriers that are mediated by anti-ILTV innate and cell-mediated immune responses (15–17), the manipulation of the cell-intrinsic barrier that is mediated by host factors that regulate the interaction between ILTV and host cells could be another promising option. Many studies have investigated herpesvirus-host interactions in humans and mice; however, little is known about these interactions in chickens. Lee et al. explored the molecular events induced by ILTV infection in host cells using publicly available high-throughput data on host transcription profiles in chicken embryo lung cells infected with a virulent ILTV strain (18). A bioinformatic analysis revealed that several genes and pathways are significantly altered by ILTV infection; these findings were validated using quantitative PCR (qPCR) assays. Their study cast the first light on the molecular nature of the host response to ILTV infection. However, the underlying molecular basis of the host response remains largely unclear, and additional studies are urgently needed to address this issue.

The proto-oncogene tyrosine-protein kinase Src (Src) was originally isolated from a chicken sarcoma, and it was the first oncogene to be identified (19). It is well-known that Src is an important factor for a wide range of biological processes, such as cell proliferation, adhesion, angiogenesis, organization of the cell skeleton, cell division, and cell death (20–24). The tyrosine kinase focal adhesion kinase (FAK) has been shown to be required for integrin-stimulated cell migration and focal adhesion formation (25–27), the disruption of which triggers apoptosis (28, 29). The interaction between Src and FAK has been shown to promote the entry of human herpes simplex virus 1 (HSV-1) into target cells (30, 31). However, to the best of our knowledge, the effects of host Src on host cell death during human or animal herpesvirus infections have never been reported, despite the fact that Src is considered to be both a survival factor (32, 33) and a death factor (33–35).

In the present study, we used Leghorn male hepatoma (LMH) cells infected with ILTV as an *in vitro* experimental model. We investigated the molecular mechanisms of host cell responses to ILTV infection using genome-wide transcriptome studies in combination with bioinformatic analyses. We also conducted functional studies to examine the interaction between host Src and FAK.

MATERIALS AND METHODS

Ethics statement. Animal experiments were approved by the Animal Ethics Committee [approval no. SYXK (Hei) 2011022] of the Harbin Veterinary Research Institute of the Chinese Academy of Agricultural Sciences (CAAS), and they were performed in accordance with ethics guidelines using approved protocols.

Experimental animals. The allantoic cavity of 9-day-old specific-pathogen-free (SPF) chicken embryos was inoculated with 100 μl of virus specimens at 1×10^4 or 1×10^5 50% tissue culture infective doses ($TCID_{50}$) per ml, as indicated below, as well as 25 to 250 ng of SU6656 (Selleckchem, Houston, TX, USA), 250 ng of PF573228 (Sigma-Aldrich, St. Louis, MO, USA), or an equal volume of dimethyl sulfoxide (DMSO). All chicken embryos were incubated at 37°C and examined daily over 5 days. The chorioallantoic membranes (CAMs), allantoic fluids, and livers were then harvested, homogenized, and subjected to three cycles of freeze-thawing. Hematoxylin and eosin (H&E) staining was performed on sections of liver samples fixed with 4% paraformaldehyde as previously described (36).

Virus strain and cell line. The LJS09 strain of ILTV (GenBank accession no. JX458822) (15) is a virulent strain of ILTV that was isolated in China, and its genome has been sequenced. It was isolated in 2009 from 6-week-old Yellow-Foot layers housed on a farm in Jiangsu Province, China, which had not been vaccinated against ILTV, and it was stored at the Harbin Veterinary Research Institute of the CAAS. This strain can be propagated in a chemically immortalized LMH cell line, in which clear cytopathic effects (CPEs) have been observed (37, 38). LMH cells were maintained in Dulbecco's modified Eagle's medium (DMEM) supplemented with 10% fetal bovine serum (FBS), 100 U/ml penicillin, 100 μg/ml streptomycin, and 2 mM L-glutamine. Cell cultures were incubated at 37°C in 5% CO_2. The Src inhibitor SU6656 and the FAK inhibitor PF573228 were used at 1 and 10 μM, respectively, for *in vitro* experiments. Control groups were treated with DMSO at the same concentrations.

RNA interference and transfection. Two short interfering RNAs (siRNAs) that specifically recognize different sequences of the *SRC* mRNA (GenBank accession no. NM_205457.2; siSRC #1, 5′-CCA AAC ACG CUG AUG GCU U-3′; siSRC #2, 5′-GCC UCC UGG AUU UCC UGA A-3′) and a control siRNA (siControl; 5′-GCA CUU GAU ACA CGU GUA A-3′), which does not have a specific target site in chickens, were used. Transfection of siRNAs was conducted using an N-TER nanoparticle siRNA transfection system (Sigma-Aldrich) according to the manufacturer's instructions.

Plaque assay. Liquid medium-based plaque assays were performed as previously described (39), with minor modifications. Briefly, LMH cells were exposed to virus that was diluted in serum-free DMEM for 3 h at 37°C in 5% CO_2 and then washed with phosphate-buffered saline (PBS). The cells were subsequently covered with DMEM containing 10% FBS, fixed with 70% ethanol at each time point postinfection indicated below, and stained with 0.1% crystal violet.

Quantitation of virus. LMH cells were infected with LJS09 at a multiplicity of infection (MOI) of 0.1. The indicated MOI was obtained according to the number of cells to be infected and the number of infectious particles, which were estimated on the basis of the numbers of PFU, which were calculated using the following formula: $TCID_{50} \times 0.59 \approx$ PFU [1 $TCID_{50}$ is equal to $-\ln(0.5)$ PFU and is approximately 0.59 PFU] (40). Levels of virus replication were determined using $TCID_{50}$ assays (40) on LMH cells and ILTV-specific qPCR assays (38) as previously described.

Flow cytometry and immunofluorescence. We conducted fluorescence-activated cell sorting (FACS) analyses using a BD FACScan flow cytometer and CellQuest software (version 4.0.2; BD, Mountain View, CA, USA). Cell death was assayed by examining cells in the sub-G_1 phase of the cell cycle via propidium iodide (PI) staining of permeabilized cells as previously described (41). Apoptosis and necrosis were assayed with annexin V-PI using an annexin V-PI staining kit (Biyuntian, China) according to the manufacturer's instructions. Immunofluorescent detection of ILTV-positive cells was conducted on cells that had been fixed with 4% paraformaldehyde overnight. Fixed cells were incubated with a rabbit polyclonal antibody against ILTV glycoprotein I (gI), followed by a secondary goat anti-rabbit antibody conjugated to fluorescein isothiocyanate (FITC) (The Jackson Laboratory, Bar Harbor, ME, USA). A polyclonal antibody against the gI of ILTV was produced in a rabbit. Briefly, the rabbit was first immunized with the pCAGGS-gI vector via intramuscular injection, followed by boosting with inactivated ILTV and recombinant gI protein via intramuscular injection. The background level of reactivity was determined using control serum from nonimmunized SPF rabbits.

Protein extraction and Western blotting. Western blotting was performed under reduced denaturing conditions according to previously described procedures (42). Antibodies against Src (EMD Millipore, Billerica, MA, USA), phosphorylated Src Tyr416 (EMD Millipore), FAK (Santa Cruz, Shanghai, China), phosphorylated FAK Tyr397 (Cell Signaling Technology, Inc. [CST], Shanghai, China), phosphorylated FAK Tyr576/577 (CST), β-actin (Sigma-Aldrich), and β-tubulin (Sigma-Aldrich) were used. The intensity of the bands was measured using ImageJ software (43).

TABLE 1 Reverse transcription-qPCR primers used for microarray data validation

Primer	Orientation[a]	Sequence (5′–3′)
ADA	F	CCAAGGTAGAACTTCACATCC
	R	TTAAGCGATAGCGGTGTTTG
CD3E	F	AGACTACGAGCCCATCAG
	R	TAGCCAGAAGCATTCAGC
PCSK5	F	AAGGATGCCACGGAAGAG
	R	ATAAGTCTACAGGAGCAGGAG
TNFRSF8	F	ATCAGAGGCACTTCAGAGAC
	R	GTTCAACTTGGCACAGTCC
IL21R	F	GCACTGTGGACATGACTGAG
	R	GAGGCTGTGGTCTGATGTTATC
CDH11	F	TGCTTGTCATTGTAGTGTTGTTTG
	R	CTTCCTCTCCTCCTCCTTCATC
NEGR1	F	GACACATCTCTCCATCTG
	R	GGGCAAAGTTTACTGTTAC
VCAN	F	AAATCACAGGCAATGATACAGATC
	R	GCATCAGTATGGGTCTCATCTAC
ASNS	F	CGGGTGAAGAAGTTCCCTTATCTG
	R	ACTGCTCCTGCAACTGTTTGAAG
DDX4	F	CACCATTACTGGCTTTTGAAGAAG
	R	TCCCGCCCTGCTTGTATAAC
ENTPD1	F	ATGCGGCTCCTCAGGTTGG
	R	TCCATCCATAGGCTCCTTCTTCC
FST	F	CTTATCCGAGCGAGTGTG
	R	GGTCTTCGTTAATGGAGTTG
NOV	F	TCTGCATGGTGCTGGAAGG
	R	GCTGGGCTGGAACGTCTC
OTC	F	CAATTATGGCTGTCATGGTTTCC
	R	GATCCAAGCATCAAAATGTAGGC
SFRP2	F	CCAGGGAAGCACCCAAAGTC
	R	GCAGAGGTTTTCCATGATGTCG
WNT7B	F	TGGGAGTTACCTAGCTTTGTCATC
	R	GGCGGCTCTGGCAGATTG
CYGB	F	AACACTGTGGTGGAGAAC
	R	CGGTGAGCTTCTTAAAGTAG
SMAD9	F	GGTTCTGCCTGGGACTGC
	R	AGATGGACACCTTTTCCTATGTG
ST6GALNAC2	F	TAACACCTCCTCCAACAC
	R	CAGCCTGAAGACCAAATC
RASSF9	F	AAACAGACCTCCCAGCAAAG
	R	GCCACATACAATCTTCTCTTCTTG

[a] F, forward; R, reverse.

Microarray analysis and qPCR assays. To profile mRNA expression in LMH cells, we used a 4 × 44K chicken gene expression microarray (catalog number 026441; Agilent Technologies, Santa Clara, CA, USA) as previously described (44). We conducted qPCR assays as described previously, using specific oligonucleotide primers (Table 1) (44). Data were analyzed with the $2^{-\Delta\Delta CT}$ threshold cycle (C_T) method, and the results are presented as the $\log_2$ fold change.

High-throughput data analysis. Microarray data were analyzed with R (http://www.r-project.org/). Gene ontology (GO) analysis and pathway analysis were performed with DAVID bioinformatics resources (gene enrichment analysis using the EASE score with a modified Fisher's exact test P value of <0.05 as the threshold) (45). Functional protein network analysis was performed with STRING software (46).

Histopathological examination. Samples of embryo livers were collected and fixed in 4% paraformaldehyde. The fixed samples were sent to the Plague Diagnosis and Technical Service Center of the Harbin Veterinary Research Institute (an animal biosafety level 3 facility accredited by the China National Accreditation Service for Conformity Assessment [CNAS]) for histopathological examination. Briefly, samples were embedded in paraffin and then sectioned. The sample slides were stained with H&E and observed by light microscopy. A histopathological examination report was provided by the Plague Diagnosis and Technical Service Center.

Statistical analysis. We used the SPSS software package (SPSS for Windows, version 13.0; SPSS Inc., Chicago, IL, USA) for statistical analysis. Data obtained from several experiments are reported as the mean ± standard deviation (SD). The difference between two groups was determined by Student's t test. One-way analysis of variance (ANOVA) with a Bonferroni correction was employed for multigroup comparisons. For all analyses, a P value of <0.05 was considered significant.

Microarray data accession number. Microarray raw data were uploaded to the National Center for Biotechnology Information Gene Expression Omnibus database under accession number GSE70855.

RESULTS

Biological characterization of ILTV-LSJ09 infection in LMH cells. The biological characteristics of ILTV-LSJ09 infection in LMH cells, including cell growth, cell death, virus replication, virus release, and virulence, were examined. ILTV infection significantly reduced the number of adherent cells that were negative for trypan blue staining by the third day postinfection (3 dpi), while cells in the control cultures continued to grow (Fig. 1A). Consistent with the reduction in the proportion of living cells following ILTV infection in our system (Fig. 1A), the proportion of apoptotic cells significantly increased from 2 dpi compared with that of control cells (Fig. 1B). The CPE of ILTV on LMH cells occurred by 2 dpi and became more severe as time progressed (Fig. 1C). In parallel with the induction of apoptosis and the occurrence of the CPE, the results of the qPCR assay showed that ILTV replicated exponentially in LMH cells from 2 dpi, whereas viral replication was not significant at 1 dpi compared with that at 0 dpi (Fig. 1C; the P values for replication at 1 and 2 dpi were 0.127 and 0.022, respectively). In addition, a concomitant, continuous increase in the copy number of the viral genome was observed in the medium from 2 dpi (Fig. 1C), which possibly explains the occurrence of the ILTV CPE at 2 dpi (Fig. 1C). The results of the qPCR assays were confirmed by $TCID_{50}$ assays (Fig. 1D). No significant CPE was observed until 2 dpi, after which the virus titer increased continually in the cells and medium (Fig. 1D). The proportion of ILTV-infected cells was determined by FACS, and it was approximately 10% at 2 dpi but only about 1.5% at 1 dpi (Fig. 1E).

Src, a central modulator of host molecular events, is induced by ILTV infection. To understand the molecular events induced by ILTV infection in LMH cells when the CPE was evident, RNA was isolated from LMH cells at 2 dpi instead of at 1 dpi. We chose this time because the proportion of virus-infected cells at 1 dpi was too low to differentiate the transcription signature of virus-infected cells from that of all cells (Fig. 1C and D). We identified 608 genes that were differentially expressed between control and ILTV-infected cells based on the following criteria: (i) a P value of <0.001 and (ii) a fold change in expression of >1.5 (data not shown). Hierarchical clustering analysis using these 608 genes demonstrated efficient clustering of biological replicates for control and ILTV-infected cells. We identified 297 downregulated genes and 311 upregulated genes following infection (Fig. 2A). For validation, the transcription levels of 20 genes which were randomly selected from the 608 genes were examined using qPCR assays. The qPCR results corresponded with those from the microarray assays (Fig. 2B).

GO analysis was performed using the DAVID functional an-

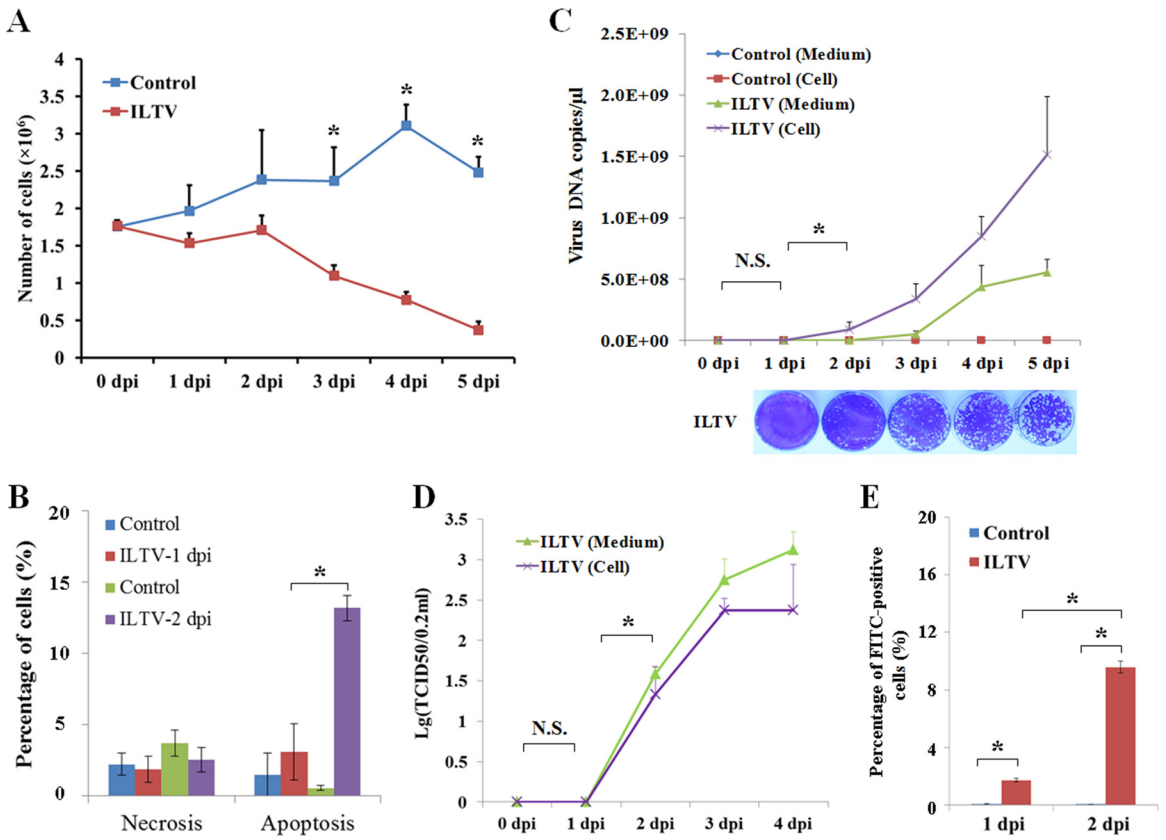

FIG 1 Biological characterization of ILTV infection in LMH cells. (A) Growth curve of LMH cells after ILTV infection. The number of adherent cells that were negative for trypan blue staining was counted. Data are presented as the mean ± SD ($n = 3$). (B) Necrosis and apoptosis of ILTV-infected LMH cells at 1 dpi and 2 dpi were assayed by flow cytometry using annexin V-propidium iodide staining. The percentage of necrotic/apoptotic cells is presented as the mean ± SD ($n = 3$); *, $P < 0.05$. (C and D) The replication of ILTV in LMH cells and the release of virus into the medium were determined by both an ILTV-specific real-time qPCR (C, top) and a $TCID_{50}$ assay (D). The cytopathic effect of ILTV infection on LMH cells was assayed by a plaque assay and visualized by crystal violet staining (C, bottom). Lg, $\log_{10}$. (E) The percentages of ILTV-infected LMH cells at 1 dpi and 2 dpi were measured by flow cytometry using a polyclonal antibody against glycoprotein I of ILTV, which was produced in SPF rabbits, followed by a fluorescein isothiocyanate-conjugated anti-rabbit second antibody. The level of background staining was determined using normal SPF rabbit serum as a control. Data are presented as the mean ± SD ($n = 3$). *, $P < 0.05$; N.S., no significant difference.

notation (subset GOTERM_CC_FAT, GOTERM_BP_FAT, and GOTERM_MF_FAT) (45) with a P value of <0.05. The five functions from each subset showing the greatest differential gene expression are listed in Fig. 2C. Cellular component analysis revealed that these differentially expressed genes were significantly enriched in those involved in the extracellular region and the plasma membrane (Fig. 2C). Meanwhile, after ILTV infection the major biological processes controlled by genes that were differentially expressed were the regulation of cell proliferation, the enzyme-linked receptor protein signaling pathway, skeletal system development, and embryonic organ development (Fig. 2C). The molecular functions of these differentially expressed genes appeared to be focused toward serine peptidase activity (Fig. 2C). Our GO analysis indicates that serine peptidase-based regulation of cell proliferation, the cytoskeleton system, and development through extra- and intracellular signal transduction may be the primary molecular events that occur in LMH cells upon ILTV infection.

To determine the central modulator of the molecular network in LMH cells after ILTV infection, we analyzed the functional connections between the proteins encoded by the 608 significant genes using STRING software with the default settings. The protein-protein interaction network was visualized by use of the Cytoscape program (47), with the layout of group attributes being done according to the degree of connectivity of the nodes (Fig. 2D). Each green rectangle represents a protein whose mRNA expression was altered by ILTV infection, and these are arranged in order of their functional connectivity to the other proteins in Fig. 2D, with the most highly connected proteins being on the top line and the least connected ones being at the bottom of Fig. 2D. Most of these nodes were directly or indirectly connected to Src, plasminogen (PLG), and serpin peptidase inhibitor, clade C (antithrombin), member 1 (SERPINC1), indicating that these three factors were the central regulators. PLG and SERPINC1 were downregulated by ILTV infection, while Src was upregulated (Fig. 2E; see also Fig. S1 in the supplemental material).

Src is a key determinant of ILTV virulence and replication in LMH cells. In ILTV-infected LMH cells, Src phosphorylation was greatly increased, although there was only a minor change in the Src protein level (Fig. 3A).

Virus-induced cell death results in extensive tissue damage during the late stages of a virulent virus infection. We sought to

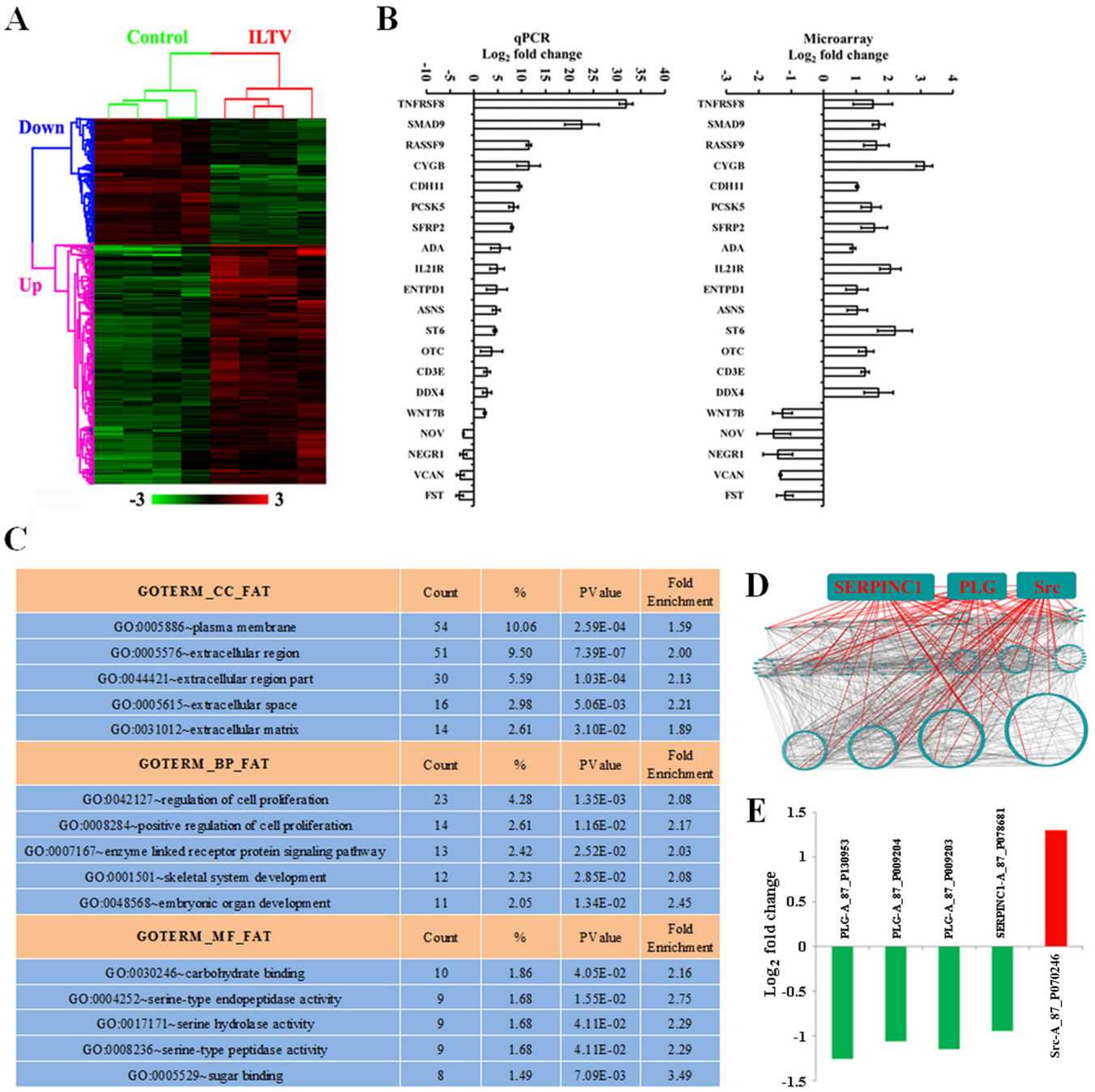

C

GOTERM_CC_FAT	Count	%	PValue	Fold Enrichment
GO:0005886~plasma membrane	54	10.06	2.59E-04	1.59
GO:0005576~extracellular region	51	9.50	7.39E-07	2.00
GO:0044421~extracellular region part	30	5.59	1.03E-04	2.13
GO:0005615~extracellular space	16	2.98	5.06E-03	2.21
GO:0031012~extracellular matrix	14	2.61	3.10E-02	1.89
GOTERM_BP_FAT	**Count**	**%**	**PValue**	**Fold Enrichment**
GO:0042127~regulation of cell proliferation	23	4.28	1.35E-03	2.08
GO:0008284~positive regulation of cell proliferation	14	2.61	1.16E-02	2.17
GO:0007167~enzyme linked receptor protein signaling pathway	13	2.42	2.52E-02	2.03
GO:0001501~skeletal system development	12	2.23	2.85E-02	2.08
GO:0048568~embryonic organ development	11	2.05	1.34E-02	2.45
GOTERM_MF_FAT	**Count**	**%**	**PValue**	**Fold Enrichment**
GO:0030246~carbohydrate binding	10	1.86	4.05E-02	2.16
GO:0004252~serine-type endopeptidase activity	9	1.68	1.55E-02	2.75
GO:0017171~serine hydrolase activity	9	1.68	4.11E-02	2.29
GO:0008236~serine-type peptidase activity	9	1.68	4.11E-02	2.29
GO:0005529~sugar binding	8	1.49	7.09E-03	3.49

FIG 2 Genome-wide transcriptome analysis to identify modulators of the host molecular events induced by ILTV infection. (A) Heat map of genes differentially expressed in LMH cells with or without ILTV infection for which P was <0.001 and the fold change in expression was >1.5. Columns indicate arrays, and rows indicate genes. Hierarchical clustering analysis identified 297 downregulated genes and 311 upregulated genes following ILTV infection. Values are normalized by row. Green, a low level of expression; red, a high level of expression. (B) The transcription of genes selected for validation of the microarray data was assayed by real-time qPCR. Both the microarray and real-time qPCR data are presented as means ± SDs ($n = 3$). (C) Gene ontology analysis of significantly differentially expressed genes ($P < 0.05$). The five functions from each subset showing the greatest differential gene expression are listed. (D) Analysis of functional interactions between the significantly differentially expressed genes reveals that Src, PLG, and SERPINC1 are the central modulators of the molecular events induced in LMH cells upon ILTV infection. (E) Average fluorescence intensities of probes targeting Src, PLG, and SERPINC1 on the microarray chip.

determine whether Src had any effect on ILTV-induced cell death using two strategies. First, the depletion of Src halted ILTV-induced Src phosphorylation at Tyr 416 (Fig. 3A), resulting in the promotion of the CPE (Fig. 3A). This effect was also evident in LMH cells that were pretreated with a well-characterized Src-specific chemical inhibitor, SU6656 (48) (Fig. 3B), which interrupts Src phosphorylation upon ILTV infection (Fig. 3B). FACS analysis of PI-stained cells found that ILTV infection in combination with the Src inhibitor resulted in levels of cell death at 2 dpi that were 4-fold higher than those in cells infected with ILTV alone

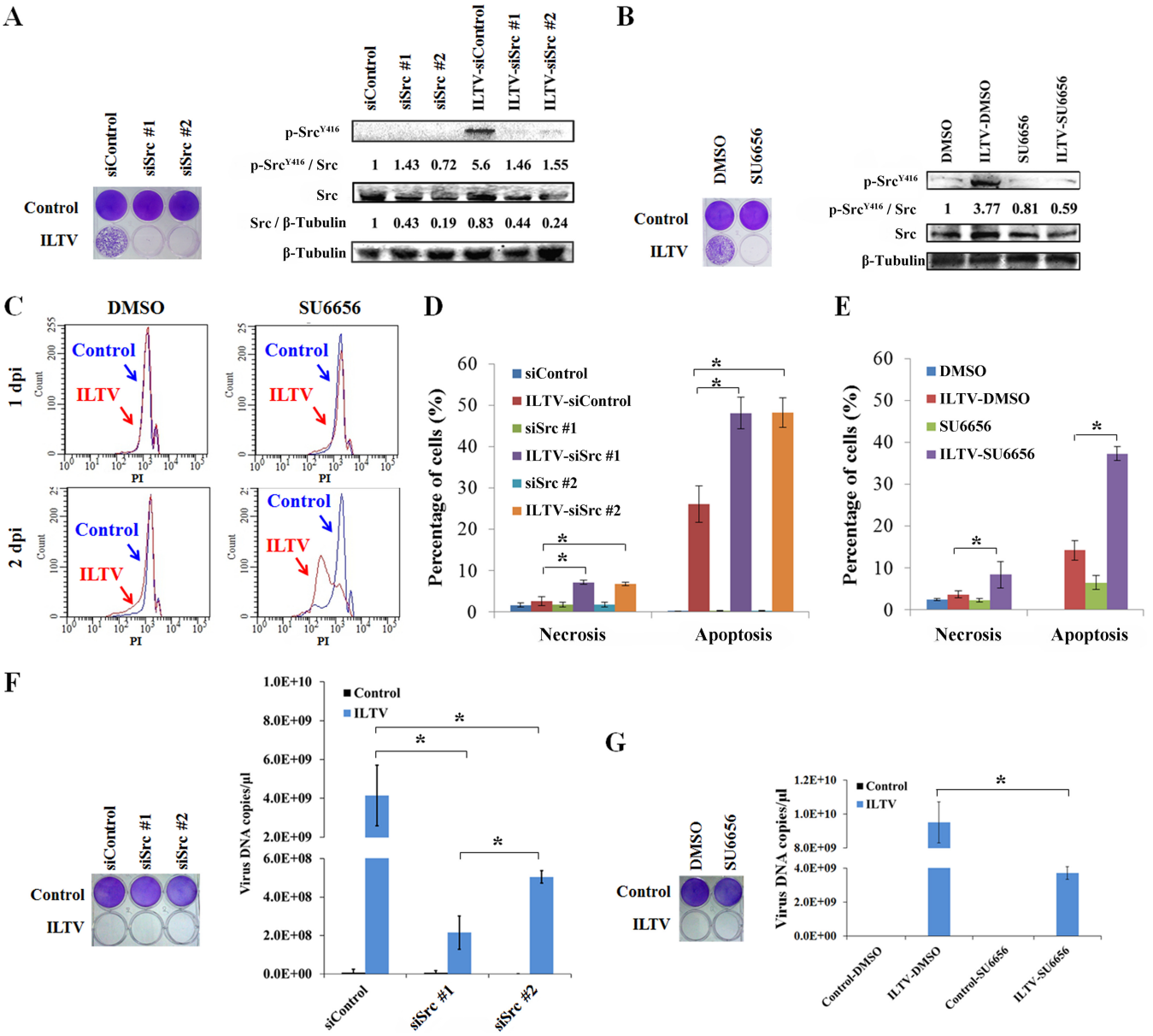

FIG 3 Inhibition of Src enhances the virulence of ILTV and limits ILTV replication in LMH cells. (A) (Right) The depletion of Src in LMH cells was performed using two siRNAs that target different Src sequences, and the protein levels of total Src and phosphorylated Src (p-SRC) were assessed by immunoblotting at day 2 after ILTV infection. β-Tubulin was used as a loading control. (Left) The depletion of Src promotes the cytopathic effect of ILTV at day 4 postinfection in LMH cells, as visualized by crystal violet staining. (B) (Right) The protein levels of total Src and phosphorylated Src in LMH cells with or without pretreatment with the Src inhibitor SU6656 at day 2 after ILTV infection were examined by immunoblotting. (Left) SU6656 promotes the cytopathic effect of ILTV at day 4 postinfection in LMH cells, as visualized by crystal violet staining. In panels A and B, the intensity ratio between the corresponding bands (upper band/lower band) was determined using ImageJ and normalized to the ratio of siControl (A) or DMSO (B). (C) Cell death was assayed by fluorescence-activated cell sorting analysis of the sub-G_1 population using PI staining. (D and E) Necrosis and apoptosis of ILTV-infected LMH cells depleted of Src or pretreated with SU6656 were assayed by flow cytometry using annexin V-PI staining. The percentage of necrotic/apoptotic cells is presented as the mean ± SD ($n = 3$). *, $P < 0.05$. (F and G) Total virus production was examined by ILTV-specific real-time quantitative PCR in LMH cells depleted of Src (F, right) or pretreated with SU6656 (G, right) when all the infected cells were dead (F and G, left). Data are presented as means ± SDs ($n = 3$). *, $P < 0.05$.

(Fig. 3C). A further detailed analysis using annexin V-PI staining revealed a significant enhancement of necrosis and apoptosis in ILTV-infected cells upon either siRNA-mediated Src depletion or the administration of SU6656 (Fig. 3D and E), thereby demonstrating that inhibition of Src promoted LMH cell death during ILTV infection. The reduced threshold of ILTV-induced cell death by Src inhibition suggests that Src prolongs the survival of LMH cells in response to ILTV infection. Along with greater ILTV virulence, inhibition of host Src by either siRNA-mediated Src depletion or the administration of SU6656 resulted in >60% reductions in virus replication (Fig. 3F and G, right), as determined by qPCR when all virus-infected cells were dead (Fig. 3F and G, left).

Src is a key determinant of ILTV virulence and replication in chicken embryos. The roles of Src during ILTV infection *in vitro*

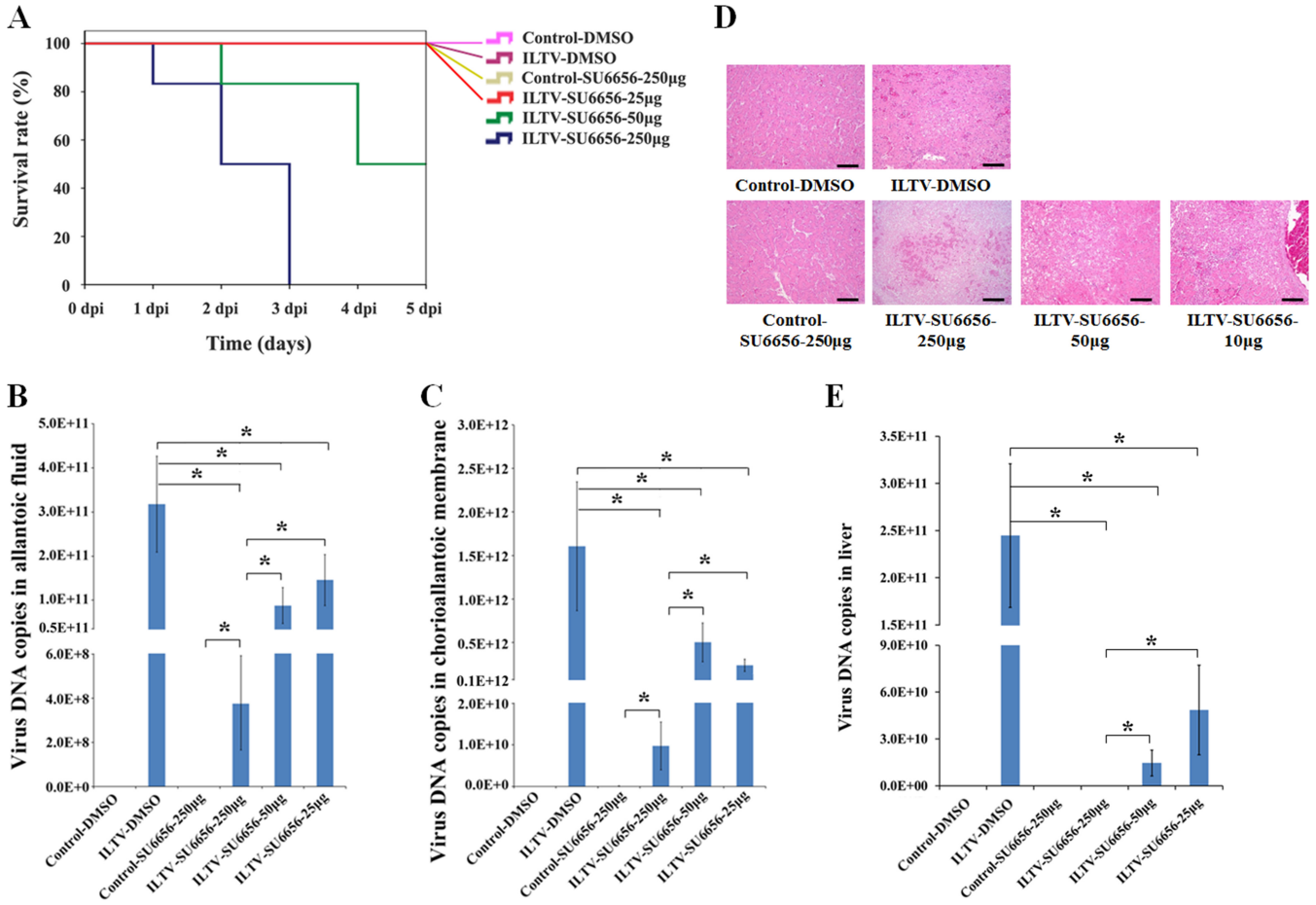

FIG 4 Dual roles of Src in ILTV infection in chicken embryos treated with serially increasing dosages of SU6656. (A) Survival analysis of embryos treated with serially increasing dosages of SU6656 ($n = 6$). (B and C) Virus production in allantoic fluid (B) and the chorioallantoic membrane (C) was detected by real-time qPCR. (D) Representative images from histopathological examinations of slides with liver tissue stained with H&E. Bars, 100 μm. (E) Virus production in the liver was detected by real-time qPCR. Data in panels B, C, and E are presented as means ± SDs ($n = 6$). *, $P < 0.05$.

were validated *in ovo* using 9-day-old SPF chicken embryos that were inoculated through the allantoic cavity with 1×10^4 $TCID_{50}$ of ILTV. Under our experimental conditions, inoculated embryo deaths occurred by 9 dpi, and all inoculated embryos were dead by 12 dpi (see Fig. S2 in the supplemental material). We first inoculated embryos with ILTV in combination with a serial dilution of the Src inhibitor SU6656. For the entire observation period (5 dpi), dead embryos were not observed at the lowest dose of SU6656 tested (25 μg). A dose of 50 μg of SU6656 resulted in the deaths of inoculated embryos by 2 dpi, with the mortality rate approaching 50% at 5 dpi (Fig. 4A). The highest dose of SU6656 (250 μg) resulted in the deaths of inoculated embryos by 1 dpi; all inoculated embryos were dead by 3 dpi (Fig. 4A). During the observation period, there were no embryo deaths in eggs treated with ILTV alone or in uninoculated eggs treated with the highest dose of SU6656 alone (Fig. 4A). Thus, the *in ovo* CPE that we observed was due to the combined effects of ILTV infection and SU6656 administration. Virus replication in allantoic fluids or CAMs was quantified by qPCR assays. Virus replication was reduced by SU6656 in a dose-dependent manner in allantoic fluids and CAMs (Fig. 4B and C).

Next, to determine whether the effects of the Src oncogene on ILTV infection that we observed in the chicken hepatoma cell line LMH could also be observed in normal liver cells, an *in ovo* examination of embryo livers was conducted. Histopathological examinations of slides with liver tissue stained with H&E revealed the infiltration of lymphocytes in all inoculated embryos (data not shown). However, different levels of hepatic tissue damage were observed among the inoculated embryos upon the administration of serially increasing dosages of SU6656. In embryos inoculated only with ILTV, necrosis was absent in four of the six samples, and mild necrosis was observed in the other two (Fig. 4D), while hepatic tissue necrosis occurred in most of the inoculated embryos upon coinoculation with SU6656 (with 25 μg of SU6656, tissue necrosis was absent in three embryos, mild in one embryo, moderate in one embryo, and severe in one embryo; with 50 μg of SU6656, tissue necrosis was absent in two embryos, mild in one embryo, moderate in one embryo, and severe in two embryos; with 250 μg of SU6656, tissue necrosis was moderate two embryos and severe in four embryos) (Fig. 4D). No necrosis was observed in the livers of either control embryos or embryos that were inoculated only with 250 μg of SU6656 (Fig. 4D). Consistent with the findings in LMH cells (Fig. 3F and G), embryo allantoic fluids (Fig. 4B), and CAMs (Fig. 4C), a dose-dependent reduction of virus

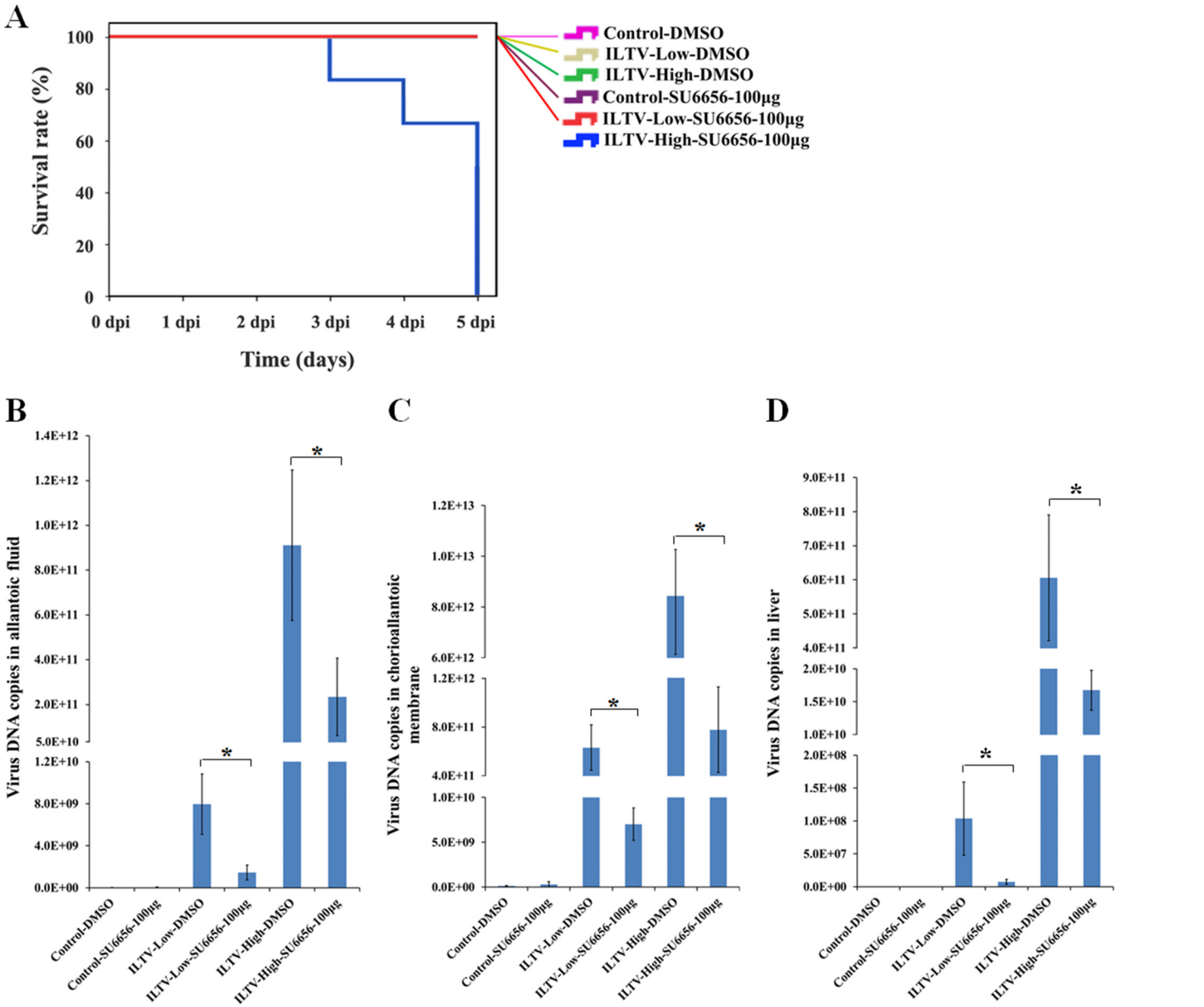

FIG 5 Dual roles of Src in ILTV infection in chicken embryos inoculated with serially increasing dosages of ILTV. (A) Survival analysis of embryos inoculated with serially increasing dosages of ILTV ($n = 6$). (B to D) Virus production in allantoic fluid (B), the chorioallantoic membrane (C), and liver (D) was detected by real-time qPCR. Low and High, low (1×10^3 $TCID_{50}$) and high (1×10^4 $TCID_{50}$) doses of ILTV, respectively. Data are presented as means ± SDs ($n = 6$). *, $P < 0.05$.

replication by SU6656 was also observed in inoculated embryos, as assayed by qPCR (Fig. 4E).

To explore the effect of virus dosage on the virulence and replication of ILTV *in ovo*, 9-day-old SPF chicken embryos were inoculated with high (1×10^4 $TCID_{50}$) or low (1×10^3 $TCID_{50}$) doses of ILTV with or without the administration of 100 μg of SU6656. All embryos inoculated with the high viral dose in the presence of 100 μg of SU6656 were dead by the end of the observation period, while no embryo deaths occurred in any other group (Fig. 5A). SU6656-mediated reductions of viral replication were observed in the allantoic fluids (Fig. 5B), CAMs (Fig. 5C), and livers (Fig. 5D) of embryos inoculated with either dose of ILTV, which rules out the possibility that SU6656 did not affect viral replication in embryos inoculated with a low dose of virus, thereby demonstrating that the difference in survival rates between the embryos inoculated with high or low doses of ILTV (in combination with 100 μg of SU6656) resulted from the different sizes of the viral inoculum.

FAK is required for Src to modulate ILTV infection in LMH cells. A pathway analysis of the subgroup of differentially expressed genes most closely connected to Src (see Fig. S3A in the supplemental material) indicated that the integrin signaling, focal adhesion, and adherens junction pathways were directly regulated by Src (see Fig. S3B in the supplemental material). Despite being involved in a wide range of biological processes (20–24), it is well-known that Src mediates integrin-focal ad-

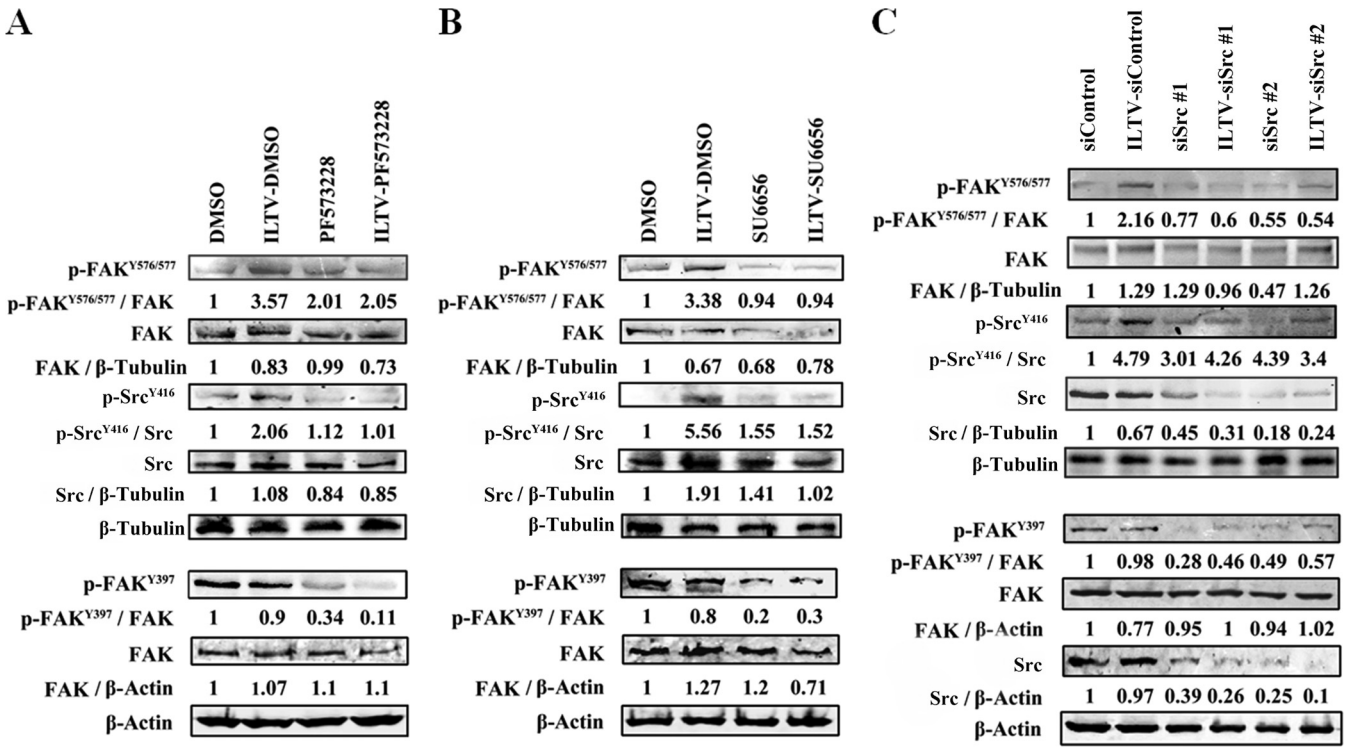

FIG 6 Interaction between Src and FAK during ILTV infection in LMH cells. (A to C) The protein levels of FAK, phosphorylated FAK (p-FAK), Src, and phosphorylated Src (p-SRC) were assayed in LMH cells with or without ILTV infection upon pretreatment with either PF573228 (A) or SU6656 (B) or upon Src depletion (C). β-Tubulin or β-actin was used as a loading control. The intensity ratio between the corresponding bands (upper band/lower band) was determined using ImageJ and normalized to the ratio of DMSO (A and B) or siControl (C).

hesion signal transduction by interacting with FAK (27, 49). Thus, we hypothesized that activated FAK is required for Src activation and the subsequent prolonged survival of LMH cells following ILTV infection.

Based on the aforementioned hypothesis, we predicted that ILTV infection would induce FAK activation in LMH cells. Immunoblotting results showed that the phosphorylation of Tyr 576/577 of FAK is enhanced by ILTV infection, although the constitutive phosphorylation of FAK at Tyr 397 and the total FAK levels were unaffected (Fig. 6A to C). In line with the essential role of the phosphorylation of FAK at Tyr 397 in the Src-mediated activation of integrin-focal adhesion signaling (26), the administration of a widely used FAK-specific chemical inhibitor, PF573228 (50), not only downregulated the constitutive phosphorylation of FAK at Tyr 397 and prevented the phosphorylation of FAK at Tyr 576/577 but also blocked the phosphorylation of Src at Tyr 416 in ILTV-infected LMH cells (Fig. 6A). These results support the involvement of FAK during ILTV infection and suggest that FAK activation is required for Src to regulate ILTV infection in LMH cells. Further immunoblotting results suggested that Src activity was indispensable for the phosphorylation of FAK at Tyr 576/577 during ILTV infection, because the phosphorylation of FAK at Tyr 576/577 during infection was prevented by pretreating the cells with either SU6656 (Fig. 6B) or specific siRNAs targeting Src (Fig. 6C). The total FAK level was not significantly affected by Src inhibition. Taken together, the findings presented above suggest that there is a positive-feedback loop between Src and FAK during ILTV infection. Additionally, the constitutive phosphorylation of FAK at Tyr 397 in LMH cells was also downregulated by SU6656 (Fig. 6B) or specific siRNAs targeting Src (Fig. 6C), indicating an essential role of basal Src activity in the maintenance of the constitutive phosphorylation of FAK at Tyr 397 in LMH cells.

Blocking FAK activity through the use of PF573228 exacerbated the ILTV CPE (Fig. 7A). The level of apoptosis induced by ILTV in cells pretreated with PF5732228 was nearly 2-fold higher than that in DMSO-treated cells at 2 dpi (Fig. 7B). In addition, ILTV replication was reduced by approximately 79% following PF573228 treatment (Fig. 7C, bottom), as assayed by qPCR when all the ILTV-infected cells were dead (Fig. 7C, top). Treatment with PF573228 *in ovo*, which did not induce embryo death by itself but which killed embryos in combination with ILTV infection during the observation period (data not shown), significantly reduced the level of virus production in allantoic fluid (Fig. 7D) and CAMs (Fig. 7E). Histopathological examinations of slides with liver tissue stained with H&E showed more severe hepatic tissue necrosis in inoculated livers upon cotreatment with PF5732228 (with ILTV infection only, tissue necrosis was absent in four inoculated livers and mild in two; with ILTV infection and PF5732228 treatment, tissue necrosis was found to be mild in one inoculated liver, moderate in three inoculated livers, and severe in two inoculated livers) (Fig. 7F). Correspondingly, a significant reduction of virus replication was observed in embryos inoculated with PF5732228 (Fig. 7G). Collectively, our *in ovo* and *in vitro* data presented above support the notion that FAK activation is indispensable for Src regulation of ILTV infection.

Taken together and consistent with our hypotheses, our results demonstrate that Src and FAK interact with each other and play a

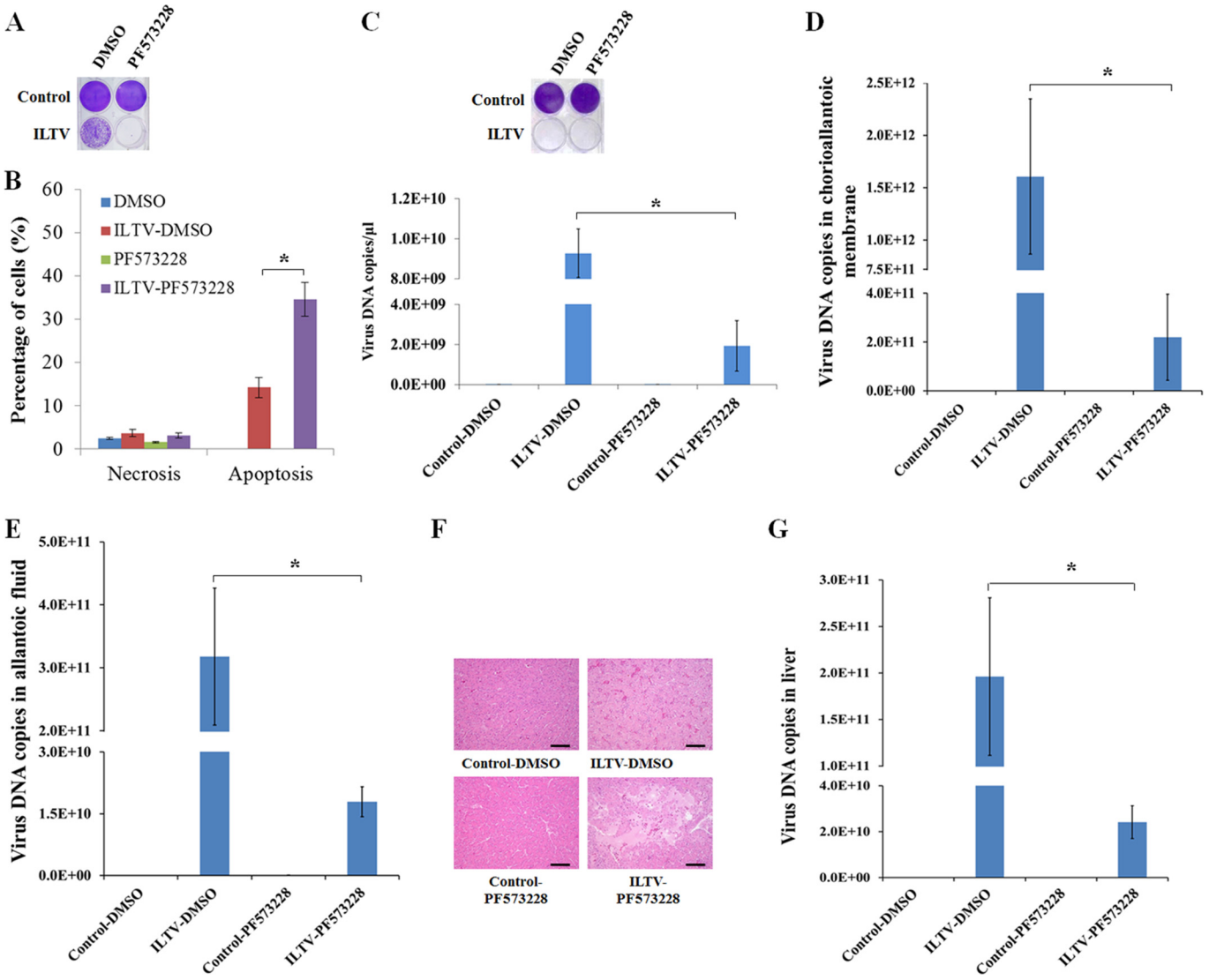

FIG 7 Inhibition of FAK enhances the virulence of ILTV and limits ILTV replication. (A) PF573228 promotes the cytopathic effect of ILTV at day 4 postinfection in LMH cells, as visualized by crystal violet staining. (B) Necrosis and apoptosis of ILTV-infected LMH cells pretreated with PF573228 were assayed by flow cytometry using annexin V-propidium iodide staining. The percentage of necrotic/apoptotic cells is presented as the mean ± SD ($n = 3$). *, $P < 0.05$. (C) (Top) PF573228 promotes the cytopathic effect of ILTV at day 4 postinfection in LMH cells, as visualized by crystal violet staining. (Bottom) Total virus production in LMH cells pretreated with PF573228 when all infected cells were dead was examined by ILTV-specific real-time qPCR. (D, E, and G) Virus production in allantoic fluid (D), the chorioallantoic membrane (E), and liver (G) was detected by real-time qPCR. Real-time qPCR data are presented as means ± SDs ($n = 6$). *, $P < 0.05$. (F) Representative images of slides with liver tissue examined histopathologically by H&E staining. Bars, 100 μm.

critical role in controlling ILTV virulence and replication *in vitro* and *in ovo*.

DISCUSSION

Targeting the host molecular network that governs the responses of host cells to ILTV infection is a promising strategy for controlling ILT in a way that is independent of host immunity. The underlying mechanisms governing ILTV-host interactions largely remain unclear, but they are important for developing novel strategies to control ILT. In the current study, we identified the Src-FAK interaction to be an essential determinant of ILTV-associated cell death in LMH cells. Based on our findings, we suggest a model where, upon ILTV infection, Src and FAK are phosphorylated and form a positive-feedback loop, thus subsequently reducing ILTV-induced host cell death but maintaining ILTV replication at high levels in host cells. However, in cells where either Src or FAK is inhibited, the phosphorylation of Src and FAK is disrupted, thereby disrupting the Src-FAK positive-feedback loop. This has the subsequent effect of enhancing the virulence of ILTV by making host cells more susceptible to ILTV-induced cell death, but it also limits ILTV replication. Furthermore, our *in ovo* studies revealed that Src inhibition induced death only in heavily infected embryos and not in embryos with mild infections, although significant reductions in the levels of viral replication were obtained in both cases (Fig. 5). We speculate that in chickens with minor ILTV infections, Src or FAK inhibition can help to quickly clear infected cells and delay disease progression, thereby limiting pathological damage. In turn, this might provide sufficient time

for the activation of a host anti-ILTV immune response, thus improving the clearance of residual infected cells. However, in chickens heavily infected with ILTV, the inhibition of host Src or FAK could exacerbate the pathological effects and even increase the likelihood of death, although viral replication might still be repressed. Further investigations of the molecular basis of the regulation of ILTV replication and ILTV-induced cell death by the Src-FAK interaction are required to develop strategies that can improve ILT control and reduce economic losses during therapy.

Src was the first oncogene identified in the Rous sarcoma virus (RSV), which infects chickens (19), and it has been implicated in multiple signaling pathways that regulate processes such as proliferation, survival, death, and angiogenesis (20–24). Src is considered to be both a survival factor (32, 33) and a death factor (33–35); however, to the best of our knowledge, the effects of host Src on host cell death in human or animal herpesvirus infections have never been reported. The findings from the present study suggest that Src contributes to the survival of host cells in response to infection with gallid herpesvirus 1 but that it is not absolutely required for virus-induced cell death (Fig. 4A to D).

In this study, we found that ILTV infection significantly promoted Src transcription but had a mild effect on the Src protein level at 2 dpi. Considering that only 10% of cells were positive for ILTV-gI staining at this time point, the difference in the expression pattern between the Src transcript and protein may be due to delayed translation of the Src transcript. We cannot rule out the possibility that oscillation of the Src mRNA/protein level or any posttranscriptional mechanism delays or even compromises the translation of additional Src transcripts. Actually, the increase in the amount of Src protein caused by ILTV infection may not be absolutely required for Src to modulate ILTV infection, because the phosphorylation of Src at Try 416, which maintains Src in an active conformation, is highly induced after ILTV infection, regardless of the absolute level of Src protein.

The interaction between Src and FAK has been shown to promote the entry of human herpes simplex virus 1 (HSV-1) into target cells (30, 31). It is possible that Src-FAK cooperation has a similar effect on the cellular entry of ILTV. This assumption is based on the observation that the Src (51) and FAK (52) protein sequences are highly conserved (>95%) among humans, mice, and chickens. It has also been shown that HSV-1 VP11/12 can directly activate a host Src family kinase (53, 54), while glycoproteins B, G, and H can activate it indirectly (55, 56). Immunoprecipitation of the Src/FAK complex, followed by proteomic sequencing in LMH cells infected with ILTV, is needed to directly identify viral proteins that interact with Src/FAK. The ability of these candidate viral proteins to activate Src/FAK can be validated by infecting LMH cells using an ILTV harboring deletions in these genes. Further integrated, genome-wide high-throughput studies combined with a functional analysis of certain host factors may be helpful in exploring the mechanism by which ILTV hijacks host Src/FAK signaling in chicken cells.

It has been well documented in humans and mice that FAK and Src function mutually in integrin-mediated signaling: autophosphorylation of FAK at Tyr 397, which is stimulated by integrin, enables FAK to bind to the SH2 domain of Src, thereby resulting in the phosphorylation of Src at Tyr 416. The phosphorylation of Src at Tyr 416 in turn promotes the phosphorylation of FAK at Tyr 576 and Tyr 577 (57–60). To uncover the interaction between Src and FAK activation in our chicken model, the phosphorylation of Src at Tyr 416 and all three related FAK tyrosine residues was detected in detail. Consistent with the prior knowledge of Src and FAK in humans and mice, the phosphorylation of FAK at Tyr 576 and Tyr 577 upon ILTV infection in our model was dependent on Src activation (Fig. 6B and C), and the phosphorylation of Src at Tyr 416 by ILTV infection also required the phosphorylation of FAK (Fig. 6A). However, the contribution of the phosphorylation of FAK at Tyr 397 to Src activation by ILTV in LMH cells is still unclear, because FAK is constitutively phosphorylated at Tyr 397 and is unaffected by ILTV infection (Fig. 6A). The basal activity of Src is also essential for the maintenance of the constitutive phosphorylation of FAK at Tyr 397 (Fig. 6A). Further investigation of the basal level of phosphorylation of FAK at Tyr 397, as well as its contribution to Src activation by ILTV in chicken cells in which FAK Tyr 397 is mutated, is required to answer this question.

Although Src activity may differ between the tumor cell line LMH and primary cells, considering the instability of the biological characteristics of different isolates and the short life span of primary cells during *in vitro* culture, the LMH cell line was chosen in the present study to establish a stable, experimental model for microarray assays and subsequent mechanistic studies. Given that the key host determinant of ILTV infection in the tumor cell line LMH is a well-known oncogene, it was crucial to determine whether the host Src/FAK-mediated mechanism that we found in LMH cells is also present in normal cells, especially *in vivo*. Hence, we first examined the effect of an Src/FAK inhibitor on ILTV replication in SPF embryos and observed an effect similar to that caused by the Src/FAK inhibitor in LMH cells (Fig. 4 and 7). Furthermore, during the *in ovo* study, we examined the histopathology of the livers of ILTV-infected chicken embryos and assayed the amount of virus transmitted to the liver. All the results support the notion that, instead of a tumor cell line-specific event, the mechanism that we identified in LMH cells is universal in normal cells and tissues. In addition, we also analyzed the only publicly available, genome-wide gene expression data for chicken embryo lung cells infected with a different virulent ILTV strain at an MOI of 0.1 (18), which again revealed that host Src is the central regulator of the molecular network induced by ILTV infection in host cells (see Fig. S4 in the supplemental material).

Vaccination using live virus is the primary method by which ILT is prevented (6). However, latent infections can still lead to outbreaks when the host immune system is compromised, such as under stress and at the onset of egg laying (13, 14, 61, 62). Therefore, novel strategies that are independent of host immunity are required to successfully control ILT. For example, the administration of therapeutic agents that target the key determinants and signaling pathways that govern the interaction between ILTV and the host at the onset of infection could reduce the extensive use of live virus-based vaccines. Here, we have uncovered a key determinant of avian ILTV infection, thereby advancing our understanding of the ILTV-host interaction. Our results also support the notion that manipulating the host molecular response can alter the biological outcomes of ILTV infection.

ACKNOWLEDGMENTS

We are greatly indebted to our colleagues who shared valuable reagents with us, and we are grateful to Xuehui Cai, Zhuo Zhang, Qimeng Tao, Liang Li, Yu Chang, Ying Yu, Gang Wang, Lijia Li, and Fei Xiao for providing technical support and valuable suggestions.

We declare no conflicts of interest.

FUNDING INFORMATION

National Twelfth Five-Year Plan for Science & Technology Support provided funding under grant number 2015BAD12B03. China Agriculture Research System provided funding under grant number CARS-41-K12. Special Fund for Agro-scientific Research in the Public Interest provided funding under grant number 201303033. Central Public-Interest Scientific Institution Basal Research Fund of China provided funding under grant number 1610302015003. Natural Science Foundation of Heilongjiang Province of China provided funding under grant number C201461. The publication reflects only the authors' views.

REFERENCES

1. **Guy JS, Barnes HJ, Smith L.** 1991. Increased virulence of modified live infectious laryngotracheitis vaccine virus following bird-to-bird passage. Avian Dis **35:**348–355. http://dx.doi.org/10.2307/1591188.
2. **Kotiw M, Wilks CR, May JT.** 1995. The effect of serial *in vivo* passage on the expression of virulence and DNA stability of an infectious laryngotracheitis virus strain of low virulence. Vet Microbiol **45:**71–80. http://dx.doi.org/10.1016/0378-1135(94)00115-D.
3. **Ou S, Giambrone JJ, Macklin KS.** 2011. Infectious laryngotracheitis vaccine virus detection in water lines and effectiveness of sanitizers for inactivating the virus. J Appl Poult Res **20:**223–230. http://dx.doi.org/10.3382/japr.2010-00300.
4. **Ou SC, Giambrone JJ, Macklin MS.** 2012. Detection of infectious laryngotracheitis virus from darkling beetles and their immature stage (lesser mealworms) by quantitative polymerase chain reaction and virus isolation. J Appl Poult Res **21:**33–38. http://dx.doi.org/10.3382/japr.2010-00314.
5. **Coppo MJ, Hartley CA, Devlin JM.** 2013. Immune responses to infectious laryngotracheitis virus. Dev Comp Immunol **41:**454–462. http://dx.doi.org/10.1016/j.dci.2013.03.022.
6. **Ou SC, Giambrone JJ.** 2012. Infectious laryngotracheitis virus in chickens. World J Virol **1:**142–149. http://dx.doi.org/10.5501/wjv.v1.i5.142.
7. **Thiry E, Meurens F, Muylkens B, McVoy M, Gogev S, Thiry J, Vanderplasschen A, Epstein A, Keil G, Schynts F.** 2005. Recombination in alphaherpesviruses. Rev Med Virol **15:**89–103. http://dx.doi.org/10.1002/rmv.451.
8. **Oldoni I, García M.** 2007. Characterization of infectious laryngotracheitis virus isolates from the US by polymerase chain reaction and restriction fragment length polymorphism of multiple genome regions. Avian Pathol **36:**167–176. http://dx.doi.org/10.1080/03079450701216654.
9. **Oldoni I, Rodríguez-Avila A, Riblet S, García M.** 2008. Characterization of infectious laryngotracheitis virus (ILTV) isolates from commercial poultry by polymerase chain reaction and restriction fragment length polymorphism (PCR-RFLP). Avian Dis **52:**59–63. http://dx.doi.org/10.1637/8054-070607-Reg.
10. **Neff C, Sudler C, Hoop RK.** 2008. Characterization of western European field isolates and vaccine strains of avian infectious laryngotracheitis virus by restriction fragment length polymorphism and sequence analysis. Avian Dis **52:**278–283. http://dx.doi.org/10.1637/8168-110107-Reg.1.
11. **Blacker HP, Kirkpatrick NC, Rubite A, O'Rourke D, Noormohammadi AH.** 2011. Epidemiology of recent outbreaks of infectious laryngotracheitis in poultry in Australia. Aust Vet J **89:**89–94. http://dx.doi.org/10.1111/j.1751-0813.2010.00665.x.
12. **Menendez KR, García M, Spatz S, Tablante NL.** 2014. Molecular epidemiology of infectious laryngotracheitis: a review. Avian Pathol **43:**108–101. http://dx.doi.org/10.1080/03079457.2014.886004.
13. **Hughes CS, Gaskell RM, Jones RC, Bradbury JM, Jordan FTW.** 1989. Effects of certain stress factors on the re-excretion of infectious laryngotracheitis virus from latently infected carrier birds. Res Vet Sci **46:**274–276.
14. **Hughes CS, Williams RA, Gaskell RM, Jordan FTW, Bradbury JM, Bennet M, Jones RC.** 1991. Latency and reactivation of infectious laryngotracheitis vaccine virus. Arch Virol **121:**213–218. http://dx.doi.org/10.1007/BF01316755.
15. **Fahey KJ, Bagust TJ, York JJ.** 1983. Laryngotracheitis herpesvirus infection in the chicken: the role of humoral antibody in immunity to a graded challenge infection. Avian Pathol **12:**505–514. http://dx.doi.org/10.1080/03079458308436195.
16. **Fahey KJ, York JJ.** 1990. The role of mucosal antibody in immunity to infectious laryngotracheitis virus in chicken. J Gen Virol **71:**2401–2405. http://dx.doi.org/10.1099/0022-1317-71-10-2401.
17. **Honda T, Okamura H, Taneno A, Yamada S, Takahashi E.** 1994. The role of cell-mediated immunity in chickens inoculated with the cell-associated vaccine of attenuated infectious laryngotracheitis virus. J Vet Med Sci **56:**1051–1055. http://dx.doi.org/10.1292/jvms.56.1051.
18. **Lee JY, Song JJ, Wooming A, Li X, Zhou H, Bottje WG, Kong BW.** 2010. Transcriptional profiling of host gene expression in chicken embryo lung cells infected with laryngotracheitis virus. BMC Genomics **11:**445. http://dx.doi.org/10.1186/1471-2164-11-445.
19. **Oppermann H, Levinson AD, Varmus HE, Levintow L, Bishop JM.** 1979. Uninfected vertebrate cells contain a protein that is closely related to the product of the avian sarcoma virus transforming gene (src). Proc Natl Acad Sci U S A **76:**1804–1808. http://dx.doi.org/10.1073/pnas.76.4.1804.
20. **Dunant N, Ballmer-Hofer K.** 1997. Signalling by Src family kinases: lessons learnt from DNA tumour viruses. Cell Signal **9:**385–393. http://dx.doi.org/10.1016/S0898-6568(97)00040-5.
21. **Parsons SJ, Parsons JT.** 2004. Src family kinases, key regulators of signal transduction. Oncogene **23:**7906–7909. http://dx.doi.org/10.1038/sj.onc.1208160.
22. **Ingley E.** 2008. Src family kinases: regulation of their activities, levels and identification of new pathways. Biochim Biophys Acta **1784:**56–65. http://dx.doi.org/10.1016/j.bbapap.2007.08.012.
23. **Tegtmeyer N, Backert S.** 2011. Role of Abl and Src family kinases in actin-cytoskeletal rearrangements induced by the Helicobacter pylori CagA protein. Eur J Cell Biol **90:**880–890. http://dx.doi.org/10.1016/j.ejcb.2010.11.006.
24. **Kinsey WH.** 2014. SRC-family tyrosine kinases in oogenesis, oocyte maturation and fertilization: an evolutionary perspective. Adv Exp Med Biol **759:**33–56. http://dx.doi.org/10.1007/978-1-4939-0817-2_3.
25. **Guan JL.** 1997. Focal adhesion kinase in integrin signaling. Matrix Biol **16:**195–200. http://dx.doi.org/10.1016/S0945-053X(97)90008-1.
26. **Beauséjour M, Thibodeau S, Demers MJ, Bouchard V, Gauthier R, Beaulieu JF, Vachon PH.** 2013. Suppression of anoikis in human intestinal epithelial cells: differentiation state-selective roles of α2β1, α3β1, α5β1, and α6β4 integrins. BMC Cell Biol **14:**53. http://dx.doi.org/10.1186/1471-2121-14-53.
27. **Mitra SK, Schlaepfer DD.** 2006. Integrin-regulated FAK-Src signaling in normal and cancer cells. Curr Opin Cell Biol **18:**516–523. http://dx.doi.org/10.1016/j.ceb.2006.08.011.
28. **Kurenova E, Xu LH, Yang X, Baldwin AS, Jr, Craven RJ, Hanks SK, Liu ZG, Cance WG.** 2004. Focal adhesion kinase suppresses apoptosis by binding to the death domain of receptor-interacting protein. Mol Cell Biol **24:**4361–4371. http://dx.doi.org/10.1128/MCB.24.10.4361-4371.2004.
29. **Lu Q, Rounds S.** 2012. Focal adhesion kinase and endothelial cell apoptosis. Microvasc Res **83:**56–63. http://dx.doi.org/10.1016/j.mvr.2011.05.003.
30. **Cheshenko N, Liu W, Satlin LM, Herold BC.** 2005. Focal adhesion kinase plays a pivotal role in herpes simplex virus entry. J Biol Chem **280:**31116–31125. http://dx.doi.org/10.1074/jbc.M503518200.
31. **Krishnan HH, Sharma-Walia N, Streblow DN, Naranatt PP, Chandran B.** 2006. Focal adhesion kinase is critical for entry of Kaposi's sarcoma-associated herpesvirus into target cells. J Virol **80:**1167–1180. http://dx.doi.org/10.1128/JVI.80.3.1167-1180.2006.
32. **Fan P, Wang J, Santen RJ, Yue W.** 2007. Long-term treatment with tamoxifen facilitates translocation of estrogen receptor alpha out of the nucleus and enhances its interaction with EGFR in MCF-7 breast cancer cells. Cancer Res **67:**1352–1360. http://dx.doi.org/10.1158/0008-5472.CAN-06-1020.
33. **Iqbal Hossain M, Hoque A, Lessene G, Aizuddin Kamaruddin M, Chu PW, Ng IH, Irtegun S, Ng DC, Bogoyevitch MA, Burgess AW, Hill AF, Cheng HC.** 2015. Dual role of Src kinase in governing neuronal survival. Brain Res **1594:**1–14. http://dx.doi.org/10.1016/j.brainres.2014.10.040.
34. **Fan P, Agboke FA, McDaniel RE, Sweeney EE, Zou X, Creswell K, Jordan VC.** 2014. Inhibition of c-Src blocks oestrogen-induced apoptosis and restores oestrogen-stimulated growth in long-term oestrogen-deprived breast cancer cells. Eur J Cancer **50:**457–468. http://dx.doi.org/10.1016/j.ejca.2013.10.001.
35. **Fan P, Griffith OL, Agboke FA, Anur P, Zou X, McDaniel RE, Creswell K, Kim SH, Katzenellenbogen JA, Gray JW, Jordan VC.** 2013. c-Src modulates estrogen-induced stress and apoptosis in estrogen-deprived breast cancer cells. Cancer Res **73:**4510–4520. http://dx.doi.org/10.1158/0008-5472.CAN-12-4152.

36. **Liu G, Wang Q, Liu N, Xiao Y, Tong T, Liu S, Wu D.** 2012. Infectious bronchitis virus nucleoprotein specific CTL response is generated prior to serum IgG. Vet Immunol Immunopathol **148:**353–358. http://dx.doi.org/10.1016/j.vetimm.2012.06.028.
37. **Kong CC, Zhao Y, Cui XL, Zhang XM, Cui HY, Xue M, Wang YF.** 2013. Complete genome sequence of the first Chinese virulent infectious laryngotracheitis virus. PLoS One **8:**e70154. http://dx.doi.org/10.1371/journal.pone.0070154.
38. **Zhao Y, Kong C, Cui X, Cui H, Shi X, Zhang X, Hu S, Hao L, Wang Y.** 2013. Detection of infectious laryngotracheitis virus by real-time PCR in naturally and experimentally infected chickens. PLoS One **8:**e67598. http://dx.doi.org/10.1371/journal.pone.0067598.
39. **Hong J, Oh HJ, Lee N, Kim DK, Yoon HS, Kim YT, Chang S, Park JH, Chung H.** 2015. Standardization of the methods and reference materials used to assess virus content in varicella vaccines. Virol J **12:**101. http://dx.doi.org/10.1186/s12985-015-0333-1.
40. **Wulff NH, Tzatzaris M, Young PJ.** 2012. Monte Carlo simulation of the Spearman-Kaerber TCID50. J Clin Bioinforma **2:**5. http://dx.doi.org/10.1186/2043-9113-2-5.
41. **Li H, Lakshmikanth T, Garofalo C, Enge M, Spinnler C, Anichini A, Szekely L, Kärre K, Carbone E, Selivanova G.** 2011. Pharmacological activation of p53 triggers anticancer innate immune response through induction of ULBP2. Cell Cycle **10:**3346–3358. http://dx.doi.org/10.4161/cc.10.19.17630.
42. **Li H, Zhang Y, Ströse A, Tedesco D, Gurova K, Selivanova G.** 2014. Integrated high throughput analysis identifies Sp1 as a crucial determinant of p53-mediated apoptosis. Cell Death Differ **21:**1493–1502. http://dx.doi.org/10.1038/cdd.2014.69.
43. **Rasband WS.** 1997–2014. ImageJ. National Institutes of Health, Bethesda, MD. http://imagej.nih.gov/ij/.
44. **Cong F, Liu X, Han Z, Shao Y, Kong X, Liu S.** 2013. Transcriptome analysis of chicken kidney tissues following coronavirus avian infectious bronchitis virus infection. BMC Genomics **14:**743. http://dx.doi.org/10.1186/1471-2164-14-743.
45. **Huang DW, Sherman BT, Lempicki RA.** 2009. Systematic and integrative analysis of large gene lists using DAVID bioinformatics resources. Nat Protoc **4:**44–57. http://dx.doi.org/10.1038/nprot.2008.211.
46. **Franceschini A, Frankild S, Kuhn M, Simonovic M, Roth A, Lin J, Minguez P, Bork P, von Mering C, Jensen LJ.** 2013. STRING v9.1: protein-protein interaction networks, with increased coverage and integration. Nucleic Acids Res **41**(Database issue):D808–D815. http://dx.doi.org/10.1093/nar/gks1094.
47. **Shannon P, Markiel A, Ozier O, Baliga NS, Wang JT, Ramage D, Amin N, Schwikowski B, Ideker T.** 2003. Cytoscape: a software environment for integrated models of biomolecular interaction networks. Genome Res **13:**2498–2504. http://dx.doi.org/10.1101/gr.1239303.
48. **Blake RA, Broome MA, Liu X, Wu J, Gishizky M, Sun L, Courtneidge SA.** 2000. SU6656, a selective Src family kinase inhibitor, used to probe growth factor signaling. Mol Cell Biol **20:**9018–9027. http://dx.doi.org/10.1128/MCB.20.23.9018-9027.2000.
49. **Huveneers S, Danen EH.** 2009. Adhesion signaling—crosstalk between integrins, Src and Rho. J Cell Sci **122**(Pt 8)**:**1059–1069. http://dx.doi.org/10.1242/jcs.039446.
50. **Cabrita MA, Jones LM, Quizi JL, Sabourin LA, McKay BC, Addison CL.** 2011. Focal adhesion kinase inhibitors are potent anti-angiogenic agents. Mol Oncol **5:**517–526. http://dx.doi.org/10.1016/j.molonc.2011.10.004.
51. **Anderson SK, Gibbs CP, Tanaka A, Kung HJ, Fujita DJ.** 1985. Human cellular src gene: nucleotide sequence and derived amino acid sequence of the region coding for the carboxy-terminal two-thirds of pp60c-src. Mol Cell Biol **5:**1122–1129. http://dx.doi.org/10.1128/MCB.5.5.1122.
52. **Whitney GS, Chan PY, Blake J, Cosand WL, Neubauer MG, Aruffo A, Kanner SB.** 1993. Human T and B lymphocytes express a structurally conserved focal adhesion kinase, pp125FAK. DNA Cell Biol **12:**823–830. http://dx.doi.org/10.1089/dna.1993.12.823.
53. **Wagner MJ, Smiley JR.** 2009. Herpes simplex virus requires VP11/12 to induce phosphorylation of the activation loop tyrosine (Y394) of the Src family kinase Lck in T lymphocytes. J Virol **83:**12452–12461. http://dx.doi.org/10.1128/JVI.01364-09.
54. **Wagner MJ, Smiley JR.** 2011. Herpes simplex virus requires VP11/12 to activate Src family kinase-phosphoinositide 3-kinase-Akt signaling. J Virol **85:**2803–2812. http://dx.doi.org/10.1128/JVI.01877-10.
55. **Martinez-Martin N, Viejo-Borbolla A, Martín R, Blanco S, Benovic JL, Thelen M, Alcamí A.** 2015. Herpes simplex virus enhances chemokine function through modulation of receptor trafficking and oligomerization. Nat Commun **6:**6163. http://dx.doi.org/10.1038/ncomms7163.
56. **MacLeod IJ, Minson T.** 2010. Binding of herpes simplex virus type-1 virions leads to the induction of intracellular signalling in the absence of virus entry. PLoS One **5:**e9560. http://dx.doi.org/10.1371/journal.pone.0009560.
57. **Schaller MD, Borgman CA, Cobb BS, Vines RR, Reynolds AB, Parsons JT.** 1992. pp125FAK a structurally distinctive protein-tyrosine kinase associated with focal adhesions. Proc Natl Acad Sci U S A **89:**5192–5196. http://dx.doi.org/10.1073/pnas.89.11.5192.
58. **Schaller MD, Hildebrand JD, Shannon JD, Fox JW, Vines RR, Parsons JT.** 1994. Autophosphorylation of the focal adhesion kinase, pp125FAK, directs SH2-dependent binding of pp60src. Mol Cell Biol **14:**1680–1688. http://dx.doi.org/10.1128/MCB.14.3.1680.
59. **Xing Z, Chen HC, Nowlen JK, Taylor SJ, Shalloway D, Guan JL.** 1994. Direct interaction of v-Src with the focal adhesion kinase mediated by the Src SH2 domain. Mol Biol Cell **5:**413–421. http://dx.doi.org/10.1091/mbc.5.4.413.
60. **Schlaepfer DD, Hanks SK, Hunter T, van der Geer P.** 1994. Integrin-mediated signal transduction linked to Ras pathway by GRB2 binding to focal adhesion kinase. Nature **372:**786–791. http://dx.doi.org/10.1038/372786a0.
61. **Bagust TJ.** 1986. Laryngotracheitis (gallid-1) herpesvirus infection in the chicken. 4. Latency establishment by wild and vaccine strains of ILT virus. Avian Pathol **15:**581–595.
62. **Rodríguez-Avila A, Oldoni I, Riblet S, García M.** 2007. Replication and transmission of live attenuated infectious laryngotracheitis virus (ILTV) vaccines. Avian Dis **51:**905–911. http://dx.doi.org/10.1637/8011-041907-REGR.1.